Bioorganic Chemistry 86 (2019) 410–419

Contents lists available at ScienceDirect

Bioorganic Chemistry

journal homepage: www.elsevier.com/locate/bioorg

# Discovery, synthesis and molecular corroborations of medicinally important novel pyrazoles; drug efficacy determinations through *in silico*, *in vitro* and cytotoxicity validations

P. Thangarasu[a], A. Manikandan[b], S. Thamaraiselvi[c,*]

[a] Research and Development Centre, Bharathiar University, Coimbatore 641046, India
[b] Department of Biotechnology, School of Bio-Sciences and Technology, VIT University, Vellore 632014, India
[c] PG & Research Department of Chemistry, Government Arts College, Coimbatore 641018, Tamil Nadu, India

ARTICLE INFO

*Keywords:*
ADMET
Anticancer
Anti-inflammation
Antioxidant
Breast cancer
Drug design
Molecular docking
Pyrazoles

ABSTRACT

As the global need for drugs getting increases, the necessity of novel and effective drugs are the need of the day. Pyrazoles are one of the active molecules in novel drug discovery. The present study deals about the synthesis of precursors 4-(4-fluorophenyl)-6-isopropyl-2-(methylsulfonyl) pyrimidine-5-carbohydrazides (**3a-m**) from methyl-4-(4-fluorophenyl)-6-isopropyl-2-(methyl sulfonyl) pyrimidine-5-carboxylate **(2)** by treating with substituted acetophenone. Further, *Vilsmeier-Haack* reaction of compounds **3a-m** at 70 °C for 8–10 hrs gave novel pyrazole carbaldehyde derivatives **(4a-m)** in good yield. Biological properties like antioxidant, anti-breast cancer and anti-inflammatory of newly synthesized compounds **(4a-m)** were determined. The enzymes Cyclooxygenase-2 and Phosphoinositide-3-Kinase are most responsible for the corresponding diseases such as inflammation and breast cancer respectively. In order to examine the interaction between these two enzymes and our synthesized compounds **4a-m**, molecular docking study was carried out. From the results, few compounds of **4a-m** were found to have anti-inflammatory properties by showing excellent COX-2 inhibition and HRBC membrane stabilization properties. ADMET prediction results were also valuable to screen the most effective pyrazole derivatives to establish them as future COX-2 inhibitors or anti-inflammatory drugs.

## 1. Introduction

Small molecules are the basis of classic drug design and development. These are achieved or synthesized by chemical reactions amid various organic/inorganic compounds [1–3]. Because of their tiny size, once consumed, the solidified active ingredients of small molecule drugs engrossed into the bloodstream reaching essentially and effectively any preferred location of the body [4]. A wide range of biological activities has been reported against pyrazole derivatives until today (Fig. 1). Pyrazole and its derivatives are one of the best and promising drug candidates [5–10]. They are anti-inflammatory, anti-microbial [8], anticancer [9,10], anti-angiogenic [11], antiviral [12], antioxidants [13] neuroprotective [14], Hypoglycemic agents [15] and platelet aggregation inhibitors [16]. In the preliminary bioactivity potential prediction assessments, present study compounds were showed a dominant and equal activity potentials against both inflammation and cancer.

To determine the most favorable bioactivity and the most potent compounds, we have proposed a few *in silico* and *in vitro* analysis to do the same. As the oxidative playing a major role in inflammation and cancers [17,18], an $H_2O_2$ radical scavenging based antioxidant (*in vitro*) activity study was carried out. HRBC membrane stabilization based study to determine the anti-inflammatory potential *in vitro*. Since cyclooxygenase 1 & 2(COX1 & 2) are highly involving in inflammation acceleration and development, the inhibitory potential of COX-1 and COX-2 by the pyrazole derivatives was aimed to be determined through a competitive ELISA based inhibition assay [19,20]. The major symptoms of inflammation and pain can be cured by the pharmacological inhibition of Cyclooxygenase [21]. The drugs which are used to do this are precise to the Cyclooxygenase-2 isozyme (COX-2) and are called COX-2 inhibitors.

In fact, a COX-2 selective inhibitor Celecoxib (4-[5-(4-methyl phenyl)-3-(trifluoromethyl)-1H-pyrazol-1-yl] benzenesulfonamide) is a diaryl-substituted pyrazole compound [22,23]. Simultaneously, the anticancer effect of the pyrazole derivatives was also proposed to be evaluated. Since the bioactivity prediction results suggested kinase inhibition as one of predominant activity (Fig. 2), a phosphoinositide

* Corresponding author.
*E-mail address:* thamaraimohan@gmail.com (S. Thamaraiselvi).

https://doi.org/10.1016/j.bioorg.2019.02.003
Received 1 December 2018; Received in revised form 17 January 2019; Accepted 2 February 2019
Available online 07 February 2019

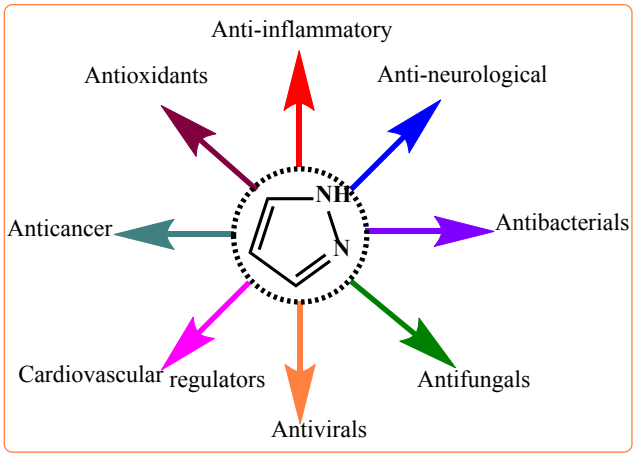


**Fig. 1.** Pyrazoles and their biological activities.

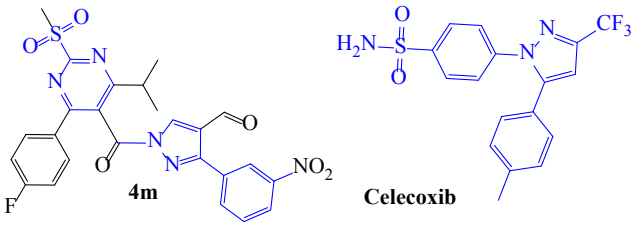


**Fig. 2.** Structural and functional group similarity between present study compounds (4 m as displayed here representative compound).

kinase-3 (PI3Kinase) inhibition and anti-breast cancer effect were evaluated for the pyrazole compounds. PI3K inhibitors are the medicinal drugs that are functioning by inhibiting one or more of the PI3-kinase enzymes, which are playing a vital role in PI3K/AKT/mTOR pathway, an imperative signaling pathway for numerous cellular functional activities such as metabolism, growth control, and translation initiation. Our research group is mainly involving in PI3Kinase inhibitor development has reported few quinoline [24–26], S-Binol [27] and imino-oxindole [28], based PI3Kinase inhibitors.

In the mechanism of development of breast cancer, PI3K/Akt/mTOR pathway plays a vital role [29,30]. The heterodimer of PI3Kinase contains two subunits, namely p85 and p110. The p85 is the regulatory subunit which is regulating the activation of the catalytic subunit (p110) in response to the absence or presence of upstream stimulation by growth factor receptor tyrosine kinases (RTKs) [31]. Moreover, chronic inflammation playing a major role in cancer development and thus a direct connection therebetween cancer and inflammation [32,33]. Actually, inflammatory breast cancer (IBC) is a rare and aggressive form of breast cancer. According to the American Cancer Society, about 1% of all breast cancer cases in the United States are inflammatory breast cancers (www.breastcancer.org/symptoms/types/inflammatory). In the mechanism, acute tumor-mediated immune responses including cytolytic T lymphocytes seem to defend against tumor progress, while immune responses involving chronic activation of humoral immunity, infiltration by Th2 cells, and protumor-polarized innate inflammatory cells result in the promotion of tumor development and disease progression [34]. Thus, the present study intended to execute the anti-inflammatory activity and along with MTT assay based cytotoxic assessments of pyrazole compounds.

## 2. Methods and materials

All organic chemicals and solvents were procured from Sigma-Aldrich, Merck and were used as received without doing further purification. Thin-Layer chromatography (TLC) was executed using pre-coated silica plates (Merck-silica gel 60 F254). Merck silica gel 60 (230–400 mesh) was used for flash column chromatography. Melting point (mp) were checked using an OptiMelt automated melting point system and are uncorrected. $^{1}$H NMR (400 MHz) and $^{13}$C NMR (100 MHz) spectra were recorded on Bruker-400 MHz instrument. Mass spectra of all compounds were recorded on Agilent ion trap MS and Infrared (IR) spectra were recorded on Perkin Elmer FT-IR spectrometer.

### *2.1. Procedure for the preparationof 4-(4-fluorophenyl)-6-isopropyl-2-(methylsulfonyl) pyrimidine-5-carbohydrazide (2)*

A mixture of the methyl 4-(4-fluorophenyl)-6-isopropyl-2-(methylsulfonyl)pyrimidine-5-carboxylate **(1)** and hydrazine hydrate (molar ratio 1:5) in ethanol was refluxed for 8–10 h. Reaction mass was cooled to 25–30 °C. Solid formed was filtered and recrystallized from ethanol. Yield 90%. Melting point: 120.3–122.1 °C. IR (KBr) : 3331, 3069, 2968, 2875, 1715, 1607, 1551, 1509, 1429, 1389, 1263, 1229, 1157, 1199, 1098, 1070, 1014, 898, 849, 799, 699, 577 cm$^{-1}$; $^{1}$H NMR: NMR (400 MHz, $CDCl_3$) $\delta$ ppm: 1.186–1.202 (d, 6H, J = 6.4), 3.04–3.11 (m, 1H), 3.58 (s, 3H), 4.35 (s, 2H, $D_2O$ exchangeable), 7.28–7.32 (t, 2H, J = 8.4), 7.60 (s, 2H), 8.65(s, 1H, $D_2O$ exchangeable).$^{13}$C NMR (100 MHz, $CDCl_3$) $\delta$ ppm: 173.75, 169.01, 164.13, 163.33, 161.67, 134.95 130.08, 130.00, 115.45, 115.24, 113.25, 52.16, 32.25, 21.46. Anal calcd for $C_{15}H_{17}FN_4O_3S$: C, 51.13; H, 4.86; F, 5.39; N, 15.90; O, 13.62; S, 9.10%. Found: C, 51.15; H, 4.85; F, 5.38; N, 15.92; O, 13.61; S, 9.09%.

### *2.2. General procedure for the preparation of carbohydrazide (3a-m)*

A mixture of compound **2** (0.01 mol) and substituted acetophenones (0.01 mol) with ethanol was refluxed with a few drops of glacial acetic acid for 10–12 h. The reaction mixture was cooled and then poured on to crushed ice and stirred well. The separated solid was filtered and recrystallized from ethanol. Yields for the compounds **3a-m** were observed as 85–90%. A complete characterization and spectral data of compounds **3a-m** are available in the supplementary information.

### *2.3. General procedure for the preparation of pyrazole-4-carbaldehydes (4a-m)*

Compounds **(3a-m)**, (0.05 mol) were dissolved in Vilsmeier- Haack reagent (DMF – 10 ml and $POCl_3$- 2 ml) and stirred at 70 °C for 8–10 h, then reduced the temperature to 25–30 °C. The contents were poured onto crushed ice and neutralised with sodium bicarbonate; the solid thus separated was filtered, washed with cold water, dried and the yield were obtained 65–70%.

#### *2.3.1. 1-(4-(4-fluorophenyl)–6-isopropyl-2-(methylsulfonyl)pyrimidine-5-carbonyl)-3-(4-hydroxy phenyl)-1H-pyrazole-4-carbaldehyde(4a)*

Off white colour solid. Melting point: 104.5–105.6 °C. IR (KBr): 3432, 2973, 1731, 1685, 1606, 1561, 1455, 1400, 1360, 1261, 1224, 1171, 1103, 1061, 979, 846 cm$^{-1}$. $^{1}$H NMR: NMR (400 MHz, $CDCl_3$) $\delta$ ppm: 1.336 to 1.350 (d, 6H, J = 5.6), 2.30 (s, 3H), 3.21 (m, 1H), 3.78 (s, 3H), 6.88–6.90 (d, 2H, J = 8.0), 7.35–7.44 (m, 2H), 7.795–7.831 (t,3H, J = 8.4), 8.03–8.05 (d,1H, J = 8.0), 9.60 (s,1H), 10.04 (s, 1H). $^{13}$C NMR (100 MHz, $CDCl_3$) $\delta$ ppm: 185.25, 175.41, 167.38, 163.77, 158.74, 154.16, 153.30, 138.42, 132.74, 130.83, 130.74, 130.23, 122.71, 122.55, 121.72, 121.24, 116.13, 115.92, 115.24, 53.18, 33.14, 21.45. Anal calcd for $C_{25}H_{21}FN_4O_5S$: C, 59.05; H, 4.16; F, 3.74; N, 11.02; O, 15.73; S, 6.31%; C, 59.04; H, 4.17; F, 3.73; N, 11.03; O, 15.72; S, 6.31%; HRMS for $C_{25}H_{21}FN_4O_5S$ Calculated 508.5244 [M + ] *m/z*, Found 508.5242.

*2.3.2. 3-(2-fluorophenyl)-1-(4-(4-fluorophenyl)-6-isopropyl-2-(methylsulfonyl) pyrimidine-5-carbonyl)-1H-pyrazole-4-carbaldehyde (4b)*

Off white colour solid. Melting point 123.5–124.6 °C. IR (KBr): 3431, 3147, 3072, 2982, 1726, 1683, 1620, 1605, 1530, 1454, 1400, 1366, 1254, 1228, 1161, 1077, 1022, 981, 867, 819, 795, 771, 645, 597, 561 $cm^{-1}$. $^1H$ NMR: NMR (400 MHz, $CDCl_3$) $\delta$ ppm: 1.321 to 1.337 (d, 6H, J = 6.4), 3.20–3.23 (m, 1H), 3.78 (s, 3H), 7.32–7.40 (m, 4H), 7.54–7.56 (m, 1H), 7.61–7.65 (m,1H), 7.78–7.79(m,2H), 9.56(s,1H), 9.97 (s, 1H). $^{13}C$ NMR (100 MHz, $CDCl_3$) $\delta$ ppm:184.82, 175.51, 167.27, 164.86, 163.77, 162.38, 160.96, 158.50, 154.10, 148.53, 136.59, 132.60, 131.59, 130.79, 124.41, 123.40, 122.71, 119.51, 116.06, 115.84, 115.56, 53.13, 33.12, 21.36. Anal calcd for $C_{25}H_{20}F_2N_4O_4S$: C 58.82; H, 3.95; F, 7.44; N, 10.97; O, 12.54; S, 6.28%. Found: C 58.80; H, 3.96; F, 7.45; N, 10.95; O, 12.53; S, 6.27%; HRMS for $C_{25}H_{20}F_2N_4O_4S$ Calculated 510.5158 [M + ] *m/z*, Found 510.5155.

*2.3.3. 3-(4-fluorophenyl)-1-(4-(4-fluorophenyl)-6-isopropyl-2-(methylsulfonyl) pyrimidine-5-carbonyl)-1H-pyrazole-4-carbaldehyde (4c)*

Off white colour solid. Melting point 128.5–129.8 °C; IR (KBr) 3432, 2971, 2869, 1721, 1693, 1605, 1561, 1543, 1454, 1392, 1256, 1223, 1160, 1100, 981, 912, 864, 773, 731, 559 $cm^{-1}$; $^1H$ NMR: NMR (400 MHz, $CDCl_3$) $\delta$ ppm: 1.335 to 1.35 (d, 6H, J = 6), 3.20–3.22 (m, 1H), 3.78 (s, 3H), 7.28–7.32 (m, 2H), 7.40–7.42 (m, 2H), 7.63–7.78 (m,2H), 7.84–8.01 (m,2H), 9.07 (s,1H), 9.55 (s,1H), 10.05 (s,1H). $^{13}C$ NMR (100 MHz, $CDCl_3$) $\delta$ ppm: 185.06, 175.44, 167.28, 164.85, 164.00, 163.73, 162.38, 161.54, 154.01, 152.35, 139.04, 132.62, 131.65, 130.78, 130.69, 127.45, 122.59, 116.08, 115.86, 115.38, 115.17, 53.14, 33.91, 33.01, 21.38. Anal calcd for $C_{23}H_{23}FN_4O_4S$: C, 58.82; H, 3.95; F, 7.44; N, 10.97; O, 12.54; S, 6.28. Found: C, 58.84; H, 3.96; F, 7.42; N, 10.96; O, 12.55; S, 6.27; HRMS for $C_{23}H_{23}FN_4O_4S$ Calculated 510.5158 [M + ] *m/z*, Found 510.5159.

*2.3.4. 3-(4-bromophenyl)-1-(4-(4-fluorophenyl)-6-isopropyl-2-(methylsulfonyl)pyramid -ine-5-carbonyl)-1H-pyrazole-4-carbaldehyde (4d)*

Off white colour solid. Melting point 140.5–141.4 °C; IR (KBr): 3432, 2971, 2869, 1721, 1693, 1605, 1561, 1543, 1454, 1392, 1256, 1223, 1160, 1100, 981, 912, 864, 773, 731, 559 $cm^{-1}$; $^1H$ NMR: NMR (400 MHz, $CDCl_3$) $\delta$ ppm: 1.33–1.34 (d, 6H), 2.49 (s, 3H), 3.21 (m, 1H), 3.77 (s, 3H), 7.42 (m, 2H), 7.60–7.70 (m, 4H), 7.78–7.92 (m,2H), 7.78–7.92 (m, 2H), 9.60 (s,1H), 10.06 (s, 1H). $^{13}C$ NMR (100 MHz, $CDCl_3$) $\delta$ ppm: 184.98, 175.46, 167.29, 164.87, 163.75, 162.39, 153.97, 152.17, 139.16, 132.61, 131.31, 130.79, 130.61, 130.17, 122.94, 122.70, 122.66, 116.09, 115.87, 53.17, 34.00, 33.14, 21.40. Anal calcd for $C_{25}H_{20}BrFN_4O_4S$: C, 52.55; H, 3.53; Br, 13.98; F, 3.32; N, 9.80; O, 11.20; S, 5.61%. Found: C, 52.57; H, 3.52; Br, 13.99; F, 3.32; N, 9.81; O, 11.22; S, 5.60%; HRMS for $C_{25}H_{20}BrFN_4O_4S$ Calculated 521.4214 [M + ] *m/z*, Found 521.4215.

*2.3.5. 3-(3-bromophenyl)-1-(4-(4-fluorophenyl)-6-isopropyl-2-(methylsulfonyl)pyramid -ine-5-carbonyl)-1H-pyrazole-4-carbaldehyde (4e)*

Off white colour solid. Melting point 124.9–125.6 °C; IR (KBr): 3434, 3070, 2973, 2872, 1727, 1697, 1604, 1561, 1523, 1449, 1390, 1269, 1220, 1158, 1098, 1012, 912, 848, 767, 741, 557 $cm^{-1}$; $^1H$ NMR : NMR (400 MHz, $CDCl_3$) $\delta$ ppm: 1.33–1.35 (d, 6H, J = 8), 2.34 (s, 3H), 3.20–3.23 (m, 1H), 3.78 (s, 3H), 7.38–7.46(m, 3H), 7.65–7.66 (d, 1H, J = 4), 7.77 (m,2H), 7.94–7.96 (d, 1H, J = 8), 8.15 (s,1H), 9.57 (s,1H), 10.04 (s, 1H). $^{13}C$ NMR (100 MHz, $CDCl_3$) $\delta$ ppm: 184.94, 175.46, 167.24, 164.86, 163.76, 162.38, 153.94, 151.71, 139.23, 133.22, 132.59, 132.11, 131.03, 130.78, 130.69, 130.44, 127.65, 122.69, 121.52, 116.07, 115.86, 53.14, 33.11, 21.38. Anal calcd for $C_{23}H_{23}FN_4O_4S$: C, 52.55; H, 3.53; Br, 13.98; F, 3.32; N, 9.80; O, 11.20; S, 5.61%. Found C, 52.57; H, 3.52; Br, 13.97; F, 3.34; N, 9.78; O, 11.21; S, 5.61%; HRMS for $C_{23}H_{23}FN_4O_4S$ Calculated 521.4214 [M + ] *m/z*, Found 521.4211.

*2.3.6. 1-(4-(4-fluorophenyl)-6-isopropyl-2-(methylsulfonyl)pyrimidine-5-carbonyl)-3-p-tolyl-1H-pyrazole-4-carbaldehyde (4f)*

Off white colour solid. Melting point 130.5–131.7 °C. IR (KBr): 3435, 3127, 2975, 2948, 2870, 1724, 1697, 1598, 1514, 1454, 1396, 1256, 1227, 1063, 981, 850, 593 $cm^{-1}$. $^1H$ NMR: NMR (400 MHz, $CDCl_3$) $\delta$ ppm: 1.33–1.346 (d, 6H, J = 6.4), 3.20–3.23 (m, 1H), 3.77 (s, 3H), 3.81(s, 3H), 7.054–7.072 (d, 1H, J = 7.2), 7.40–7.42 (m, 3H), 7.50–7.53 (m,2H), 7.77–7.80 (m, 2H), 9.55 (s,1H), 10.06 (s, 1H). $^{13}C$ NMR (100 MHz, $CDCl_3$) $\delta$ ppm: 185.21, 175.44, 167.34, 164.87, 163.78, 154.14, 153.64, 139.05, 138.43, 132.70, 130.83, 130.74, 128.99, 128.64, 128.17, 122.71, 122.64, 116.15, 115.93, 53.19, 34.08, 33.13, 21.45. Anal calcd for $C_{26}H_{23}FN_4O_4S$: C, 61.65; H, 4.58; F, 3.75; N, 11.06; O, 12.63; S, 6.33%; Found C, C, 61.67; H, 4.55; F, 3.76; N, 11.05; O, 12.64; S, 6.32%; HRMS for $C_{26}H_{23}FN_4O_4S$ Calculated 506.5524 [M + ] *m/z*, Found 506.5523.

*2.3.7. 3-(4-chlorophenyl)-1-(4-(4-fluorophenyl)-6-isopropyl-2-(methylsulfonyl)pyrimidi -ne-5-carbonyl)-1H-pyrazole-4-carbaldehyde (4 g)*

Off white colour solid. Melting point 135.5–136.8 °C. $^1H$ NMR : NMR (400 MHz, $CDCl_3$) $\delta$ ppm: 1.344–1.36 (s, 6H, J = 6.4), 2.53 (s, 3H), 3.19–3.24 (m, 1H), 3.78 (s, 3H), 7.42–7.46 (t, 3H, J = 8.8), 7.578–7.598 (d, 2H, J = 8.0), 7.78–7.81 (m,2H, J = 7.6), 8.01–8.03 (d, 2H, J = 10), 9.63(s,1H), 10.08 (s, 1H). $^{13}C$ NMR (100 MHz, $CDCl_3$) $\delta$ ppm: 184.93, 175.45, 167.29, 164.87, 163.73, 162.39, 153.96, 152.03, 139.11, 134.19, 132.61, 132.58, 130.78, 130.69, 130.34, 130.16, 129.78, 128.34, 127.50, 122.66, 116.06, 115.84, 53.14, 34.04, 33.13, 21.38. Anal calcd for $C_{25}H_{20}ClFN_4O_4S$: C, 56.98; H, 3.83; Cl, 6.73; F, 3.61; N, 10.63; O, 12.14; S, 6.08%. Found: C, 56.99; H, 3.84; Cl, 6.71; F, 3.60; N, 10.64; O, 12.15; S, 6.09%; HRMS for $C_{25}H_{20}ClFN_4O_4S$ Calculated 526.9274 [M + ] *m/z*, Found 526.9272.

*2.3.8. 3-(3-chlorophenyl)-1-(4-(4-fluorophenyl)-6-isopropyl-2-(methylsulfonyl)pyrimidi -ne-5-carbonyl)-1H-pyrazole-4-carbaldehyde (4 h)*

Off white colour solid. Melting point 137.5–138.8 °C. IR (KBr): 3436, 3147, 3075, 2976, 2873, 1727, 1697, 1604, 1561, 1450, 1391, 1353, 122, 1099, 1064, 864, 848, 723, 711, 558 $cm^{-1}$.$^1H$ NMR: NMR (400 MHz, $CDCl_3$) $\delta$ ppm: 1.345–1.361 (d, 6H, J = 6.4), 3.21–3.24 (m, 1H), 3.78 (s, 3H), 7.411–7.454 (t, 2H, J = 8.4), 7.52–7.556 (d, 2H, J = 6.4), 7.782–7.814 (t,2H, J = 6.0), 7.935–7.950 (d,1H, J = 6.0), 8.04 (s, 1H), 9.62 (s,1H), 10.07 (s, 1H). $^{13}C$ NMR (100 MHz, $CDCl_3$) $\delta$ ppm: 185.09, 175.49, 167.36, 164.86, 163.86, 162.39, 154.00, 151.82, 139.40, 133.06, 132.64, 130.81, 130.30, 129.28, 128.25, 127.30, 122.75, 116.13, 115.92, 53.18, 33.12, 21.42. Anal calcd for $C_{25}H_{20}ClFN_4O_4S$: C, 56.98; H, 3.83; Cl, 6.73; F, 3.61; N, 10.63; O, 12.14; S, 6.08%. Found: C, 56.97; H, 3.82; Cl, 6.73; F, 3.59; N, 10.64; O, 12.15; S, 6.09%; HRMS for $C_{25}H_{20}ClFN_4O_4S$ Calculated 526.9274 [M + ] *m/z*, Found 526.9276.

*2.3.9. 1-(4-(4-fluorophenyl)-6-isopropyl-2-(methylsulfonyl)pyrimidine-5-carbonyl)-3-phenyl-1H-pyrazole-4-carbaldehyde (4i)*

Off white colour solid. Melting point 147.5–148.4 °C.$^1H$ NMR : NMR (400 MHz, $CDCl_3$) $\delta$ ppm: 1.345–1.362 (d, 6H, J = 6.8), 3.20–3.25 (m, 1H), 3.79 (s, 3H), 7.41–7.45 (m, 2H), 7.51–7.52 (m, 3H), 7.78–7.82(m,2H), 7.94–7.95(m, 2H),9.57 (s,1H), 10.08 (s, 1H). $^{13}C$ NMR (100 MHz, $CDCl_3$) $\delta$ ppm: 185.16, 175.46, 167.32, 164.87, 163.76, 162.39, 154.12, 153.61, 138.45, 132.68, 131.00, 130.82, 130.72, 129.42, 128.74, 128.40, 122.72, 116.13, 115.91, 53.18, 33.12, 21.43. Anal calcd for $C_{25}H_{21}FN_4O_4S$: C, 60.97; H, 4.30; F, 3.86; N, 11.38; O, 12.99; S, 6.51% ; Found C, 60.98; H, 4.31; F, 3.85; N, 11.34; O, 12.98; S, 6.52%; HRMS for $C_{25}H_{21}FN_4O_4S$ Calculated 492.5254 [M + ] *m/z*, Found 492.5253.

*2.3.10. 1-(4-(4-fluorophenyl)-6-isopropyl-2-(methylsulfonyl)pyrimidine-5-carbonyl)-3-(3-methoxy phenyl)-1H-pyrazole-4-carbaldehyde (4j)*

Off white colour solid. Melting point 147.5–148.4 °C.$^1$H NMR : NMR (400 MHz, $CDCl_3$) $\delta$ ppm: 1.33–1.346 (d, 6H, J = 6.4), 3.20–3.23 (m, 1H), 3.77 (s, 3H), 3.81(s, 3H), 7.054–7.072 (d, 1H, J = 7.2), 7.40–7.42 (m, 3H), 7.50–7.53 (m,2H), 7.77–7.80 (m, 2H), 9.55 (s,1H), 10.06 (s, 1H). $^{13}$C NMR (100 MHz, $CDCl_3$) $\delta$ ppm: 185.17, 175.46, 167.33, 164.88, 163.76, 159.145, 154.09, 153.42, 138.47, 132.67, 132.23, 130.83, 130.74, 129.54, 122.79, 122.66, 120.96, 116.13, 115.91, 114.96, 114.35, 55.16, 53.19, 34.01, 33.13, 21.42. Anal calcd for $C_{26}H_{23}FN_4O_5S$: C, 59.76; H, 4.44; F, 3.64; N, 10.72; O, 15.31; S, 6.14%; Found C, 59.77; H, 4.45; F, 3.63; N, 10.71; O, 15.30; S, 6.15%; HRMS for $C_{26}H_{23}FN_4O_5S$ Calculated 522.5514 [M + ] *m/z*, Found 522.5511.

*2.3.11. 1-(4-(4-fluorophenyl)-6-isopropyl-2-(methylsulfonyl)pyrimidine-5-carbonyl)- 3-(2-methoxy phenyl)-1H-pyrazole-4-carbaldehyde (4 k)*

Off white colour solid. Melting point 147.5–148.4 °C.$^1$H NMR: NMR (400 MHz, $CDCl_3$) $\delta$ ppm: 1.33–1.34(d, 6H, J = 4.0), 3.20–3.23 (m, 1H), 3.75 (s, 3H), 3.79 (s, 3H), 7.07–7.11 (m, 1H), 7.17–7.19 (d, 1H, J = 8.0), 7.40–7.44 (m,2H), 7.48–7.53 (m,2H), 7.78–7.81 (m, 2H), 9.38(s,1H), 9.84 (s, 1H). $^{13}$C NMR (100 MHz, $CDCl_3$) $\delta$ ppm:185.51, 175.45, 167.37, 163.70, 162.39, 157.00, 154.28, 152.10, 134.11, 132.70, 131.05, 130.59, 123.69, 122.47, 120.48, 120.16, 116.09, 115.87, 111.53, 55.46, 53.16, 33.11, 21.41. Anal calcd for $C_{26}H_{23}FN_4O_5S$: C, 59.76; H, 4.44; F, 3.64; N, 10.72; O, 15.31; S, 6.14%; Found C, 59.77; H, 4.45; F, 3.63; N, 10.71; O, 15.30; S, 6.15%; HRMS for $C_{26}H_{23}FN_4O_5S$ Calculated 522.5514 [M+] *m/z*, Found 522.5514.

*2.3.12. 1-(4-(4-fluorophenyl)-6-isopropyl-2-(methylsulfonyl)pyrimidine-5-carbonyl)-3-(4-nitrophenyl)-1H-pyrazole-4-carbaldehyde (4l)*

Yellow colour solid. Melting point 180.5–181.4 °C. IR (KBr): 3435, 3136, 2975, 2878, 1726, 1693, 1561, 1529, 1450, 1392, 1343, 1259, 1225, 1162, 1065, 864, 775, 712 $cm^{-1}$. $^1$H NMR: NMR (400 MHz, CDCl3) $\delta$ ppm: 1.355–1.371(d, 6H, J = 6.4), 3.17–3.26 (m, 1H),3.76 (s, 3H), 7.46–7.41 (t, 2H, J = 8.8), 7.82–7.79 (m, 2H), 8.281–8.259 (d,2H, J = 8.8), 8.376–8.354(d, 2H, J = 8.8), 9.69 (s,1H), 10.12 (s, 1H). $^{13}$C NMR (100 MHz, CDCl3) $\delta$ ppm: 185.08, 175.55, 167.27, 164.92, 163.82, 162.44, 153.95, 151.65, 147.75, 139.88, 137.31, 132.59, 130.85, 130.76, 129.88, 123.54, 123.03, 122.91, 116.17, 115.95, 53.24, 33.16, 21.45.0 Anal calcd for $C_{25}H_{20}FN_5O_6S$: C, 55.86; H, 3.75; F, 3.53; N, 13.03; O, 17.86; S, 5.97%; Found C, 55.88; H, 3.73; F, 3.52; N, 13.04; O, 17.85; S, 5.98%; HRMS for $C_{25}H_{20}FN_5O_6S$ Calculated 537.5224 [M+] *m/z*, Found 537.5225.

*2.3.13. 1-(4-(4-fluorophenyl)-6-isopropyl-2-(methylsulfonyl)pyrimidine-5-carbonyl)-3-(3-nitrophenyl)-1H-pyrazole-4-carbaldehyde (4 m)*

Yellow colour solid. Melting point 191.1–192.6 °C. IR (KBr): 3438, 3130, 2971, 2870, 1720, 1698, 1564, 1530, 1455, 1385, 1349, 1260, 1235, 1170, 869, 771, 705 $cm^{-1}$. $^1$H NMR : NMR (400 MHz, CDCl3) $\delta$ ppm: 1.332–1.346 (d, 6H, J = 5.6), 3.18–3.21 (m, 1H), 3.77 (s, 3H), 7.339–7.378(t, 2H, J = 8), 7.691–7.747 (m, 3H), 8.207–8.225 (d,2H, J = 7.2), 9.54 (s,1H), 10.01 (s, 1H). $^{13}$C NMR (100 MHz, CDCl3) $\delta$ ppm: 184.69, 175.45, 167.15, 164.84, 163.64, 162.35, 153.72, 150.67, 147.58, 139.79, 134.65, 132.38, 130.60, 129.69, 123.80, 123.01, 122.67, 115.91, 115.69, 53.00, 33.08, 21.25. Anal calcd for $C_{25}H_{20}FN_5O_6S$: C, 55.86; H, 3.75; F, 3.53; N, 13.03; O, 17.86; S, 5.97%; Found C, 55.87; H, 3.74; F, 3.51; N, 13.05; O, 17.85; S, 5.98%; HRMS for $C_{25}H_{20}FN_5O_6S$ Calculated 537.5224 [M+] *m/z*, Found 537.5227.

## 2.4. Molecular docking studies

### 2.4.1. Molecular docking software and tools

Molecular docking investigation was done using Autodock version 4.2.6 and Autodock Tools (ADT) version 1.5.6. Previously reported molecular docking protocols with necessary modifications were used for this study [35–39]. The 3D atomic coordinates of pyrazole derivatives (**4a-m**) were developed using ChemDraw version 15.0. Physical geometry of the compound (**4a-m)** was adjusted to exact bond length, bond angle and saved as corresponding ligands in *pdb* file format.3D crystal structure of COX-2 otherwise known as (prostaglandin synthase-2) (PDB ID: 1CX2) and PI3 Kinase (PDB ID: 1CHW) retrieved from PDB(protein data bank) (www.rcsb.org). The retrieved 3D X-ray crystallographic PDB receptors were initially processed in Arguslab software (Version 4.0.1) to remove water moieties, heteroatoms, miscellaneous molecules, and ligands if any.

### 2.4.2. The general protocol for the execution of molecular docking

Gridbox, *pdbqt* files of ligands and receptor protein was executed using AutoDock Tools (ADT), a Graphical User Interface (GUI) program. The Gridmap belongs to grid box were generated using the AutoGrid option available in the software. The grid box parameter was set as 72 × 74 × 72 xyz points (grid spacing value 0.375 Å) and the grid centers x, y, and z were set as 0.728, 0.918 and 0.860 respectively [40]. After docking the ligands (**4a-m**) into the active sites of inflammation associated COX-2 (PDB ID: 1CX2) and breast cancer associated PI3 Kinase (PDB ID: 1CHW). Statistical mechanical value analysis of the docked pyrazole derivatives (**4a-m**) was done by ranking the compounds using their obtained lowest binding energy (kcal/mol), inhibitory constant (*ki*) values and ligand efficiency [41] which were retrieved from best-docked poses. Molecular interactions such as non-covalent interactions including π-π interaction, and π-cation interaction and hydrogen bonding interaction details were assessed and evaluated for the SAR (Structure-Activity Relationships) analysis.

## 2.5. Cyclooxygenase-2 enzyme inhibition assay

A 96 well, competitive ELISA based COX-2 enzyme inhibition assay was executed in order to achieve the COX-2 inhibitory capabilities of pyrazoles **4a-m**. COX-2 activity was examined by four repeated inhibition assays (n = 4) as previously reported by Copeland *et al.* 1994, with essential adjustments [42]. N, N, N, *N*-tetra methyl-p-phenylenediamine (TMPD) oxidation during the reduction of Prostaglandin G2 (PGG2) to Prostaglandin H2 (PGH2) was taken as the parameter to determine the COX-2 inhibitory effect of pyrazole derivatives [43]. As displayed in Fig. 3, due to the functional and structural group similarity between **4a-m** and Celecoxib, an established COX-2 inhibitor, was used as the standard drug.

Namely, the aromatic azaarene, aromatic arene, and phenyl ring; dinitro comprising pyrazole rings, and leaving groups are reciprocally prevailing both in **4a-m** and Celecoxib (Fig. 2**)**. In the bioactivity investigations, initially, the bio-assay complex was pre-incubated at 20–22 °C for 60 s along with the pyrazole compounds. Then, the reaction mixture and COX-2 enzyme were supplied with EDTA (3 mM), Tris–HCl buffer (100 mM, pH 8.0), and haematin (15 mM). Arachidonic acid (ARA) and TMPD were supplied to make reaction mixture total volume of 0.25 ml. The rate of TMPD oxidation was calculated (in 20 s)

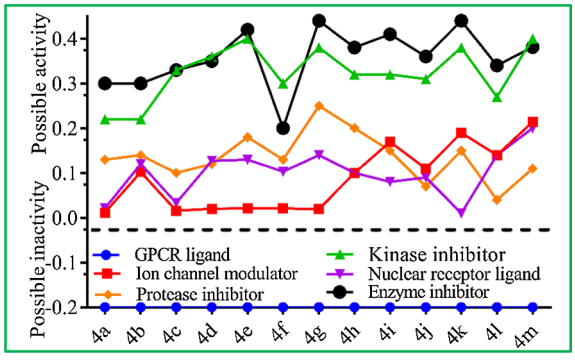


**Fig. 3.** Bioactivity prediction results of pyrazole derivatives **4a-m.**

which was considered as the enzyme activity at an absorbance wavelength of 602 nm. The inhibition percentage activity was calculated by subtracting the oxidation value in presence of TMPD to the non-enzymatic oxidation without COX-2.

### 2.6. PI3 Kinase activity assay

Glutathione-coated 96 well plate was used to perform the PI3 Kinase inhibition assay as reported previously with minor adjustments [25,27]. Before adding PIP2 (Phosphatidylinositol bisphosphate) substrate, kinase and the pyrazole compounds in different concentrations was pre-incubated for 15 min. Then, 10 µL/well of 5X Kinase reaction buffer along with 10 µL/well of PIP2 substrate was mixed. The final volume was adjusted to 50 µL/well using distilled water. Then the reaction mixture was incubated at 37 °C for 60 min. Then, 50 µL/well of Biotinylated-Phosphatidylinositol bisphosphate (b-PIP3)/EDTA working solution without the buffer control wells and 50 µL/well 1X TBS (Tris-buffered saline) to the buffer control wells were added. Then, 100 µL/well of General Receptor for Phosphoinositides 1 (GRP1) working solution was added to all wells and incubated at RT for 1 h. The wells are splashed at least 5 times with 200 µL/well 1X TBST (Tris-Buffered Saline and Tween 20) and 50 µL/well SA-HRP working solution was added and incubated at RT for 1 h. 200 µL of 1X TBST per well, then 2 times with 200 µL of 1X TBS per well was added. Finally, 100 µL of the Substrate TMB per well, developed in the dark for 5–20 min then read at 450 nm. The relative % to b-PIP3 was calculated using the following formula,

$$\%\text{inhibition} = \frac{\text{OD of samples (buffer, kinase \& inhibitors)}}{\text{OD of B} - \text{PIP3 aberage}} \times 100$$

### 2.7. Hydrogen peroxide ($H_2O_2$) radical scavenging assay

Most of the pharmaceuticals and supplements possessing antioxidant potentials may interfere with the efficiency of positive anticancer drug efficacy [44]. Thus, prior to testifying the cytotoxicity/anticancer effects of compounds **4a-m**, antioxidant potentials of pyrazoles **4a-m** was assessed through $H_2O_2$ scavenging activity evaluations [45]. The experiment was performed in triplicate and Ascorbic acid was used as a standard antioxidant. Pyrazoles **4a-m** and the standard, Ascorbic acid, were assessed in various concentration ranges (10–150 µg/mL). Prepared compound solutions were incubated after adding 0.6 ml of freshly prepared 40 mM $H_2O_2$ at 37 °C for 60 min. Absorbance was taken at 230 nm to determine the relative $H_2O_2$ scavenging activity percentage decrease of pyrazoles **4a-m**. The relative % scavenging determination of $H_2O_2$ and ascorbic acid were determined by the following formula:

$$\%H_2O_2\text{reducingactivity} = [OD_1 - OD_2/OD_1] \times 100$$

where $OD_1$ is the optical density (OD) of the control and $OD_2$ is the absorbance (OD) of **4a-m**.

### 2.8. Cytotoxicity studies on breast cancer cell lines - MTT assay

The early passage Michigan Cancer Foundation-7 (MCF-7) and MCF 10, a non-tumorigenic epithelial cell line, was used in this study [25,27]. Cells were cultured in Dulbecco's Modified Eagle's Medium (DMEM) supplemented with (100U) 20 µg/ml penicillin, 10% Fetal Bovine Serum (FBS), and 100 µg/ml streptomycin. Normal breast epithelial cells were cultured in 1:1 mixture of DMEM and Ham's F12 medium with100 µg/ml cholera toxins, 20 mg/ml of epidermal growth factor (EGF), and 500 µg/ml hydrocortisone, 0.01 mg/ml insulin, and 5% chelex treated horse serum. For the cytotoxicity assay, 1 ml of homogenized cell suspension was dispensed in each well of a microtiter plate and kept in a desiccator under 5% $CO_2$ atmosphere. The cells were observed under the inverted microscope after 48 h of incubation. 0.05 ml of the most effective candidate drugs (compounds among **4a-m**) was dissolved in 4.95 ml of DMSO to get a working concentration of 1 mg/ml. The working concentration was prepared freshly and filtered through 0.45-µm filter before bioassay.

The cytotoxicity effects most effective compounds among **4a-m** on MCF-7 cells and MCF 10 cells was determined by the 3-(4,5-dimethylthiazol-2yl)-2,5-diphenyl tetrazolium bromide (MTT) assay [25,27]. Different concentrations of candidate drugs **(4a-m)** (25–250 µg/mL) was prepared and used for the assay. In 96 well flat-bottom titer plates, approximately 5000 cells were seeded and incubated for the various time course of 24–72 h along with the compounds in various concentrations at 37 °C in 5% $CO_2$ atmosphere. After incubated, the medium was removed and the wells were washed with PBS; 100 µL of the working MTT dye in DMEM (Dulbecco's Modified Eagle's Medium) media was added and incubated for 2 h. MTT lysis buffer (100 µL) was added and incubation continued for 4 h more. The absorbance was measured at 570 nm and the cell viability was calculated using the following formula,

$$\text{Cellviability}(\%) = \text{MeanOD/ControlOD} \times 100\%$$

### 2.9. In vitro anti-inflammatory activity of pyrazoles 4a-m

Since HRBC has similar membrane structure/nature to lysosomal membrane, HRBC membrane stabilization study was carried out to ensure the ability of **4a-m** to maintain the stability of HRBC membrane which is supposed to stop the inflammatory progression by controlling the release of lysosomal enzymes [46]. Different products that are released by a lysosomal enzyme in inflammation progression generating multiple disorders and this extracellular activity are known as the acute or chronic inflammation. NSAIDs are inhibiting these lysosomal enzymes by easing the lysosomal membrane. In this study, as testified earlier, *in vitro* anti-inflammatory activity was carried out by means of Human Red Blood Cell (HRBC) membrane stabilization method (n = 4) using Diclofenac as standard [19,20]. The percentage hemolysis was calculated by assuming the hemolysis produced in presence of distilled water at 100%. The percentage of HRBC membrane stabilization was calculated using the following formula,

$$\%\text{ inhibition of hemolysis} = 100 \times [(OD_1 - OD_2)/OD_1]$$

Where $OD_2$ = optical density of sample $OD_1$ = optical density of control.

### 2.10. Statistical analysis

All results were expressed as percentage decrease with respect to control values and compared by one-way ANOVA with Dunnett's post test was performed. GraphPad Prism version 6.07 for Windows, GraphPad Software, San Diego California USA, www.graphpad.com was used for statistical analysis. A difference was considered statistically significant if $p \leq 0.05$. The 50% inhibitory concentration ($IC_{50}$) was calculated from the dose-response curve obtained by plotting percentage inhibition versus concentrations.

## 3. Results and discussion

### 3.1. Synthesis of substituted Pyrazole-4-carbaldehydes (4a-m):

Our synthetic study **(**Scheme 1**)** was initiated with the preparation of starting compound methyl 4-(4-fluorophenyl)-6-isopropyl-2-(methylsulfonyl)pyrimidine-5-carboxylate **(1)** as per the Patent WO2007/74391 A2 [47]. The treatment of **1** with hydrazine hydrate in the presence of ethanol as a solvent formed compound 4-(4-fluorophenyl)-6-isopropyl-2-(methylsulfonyl) pyrimidine-5-carbohydrazide **(2)**. Conversion of compound **2** to the precursor's **3a-m** was easily achieved by

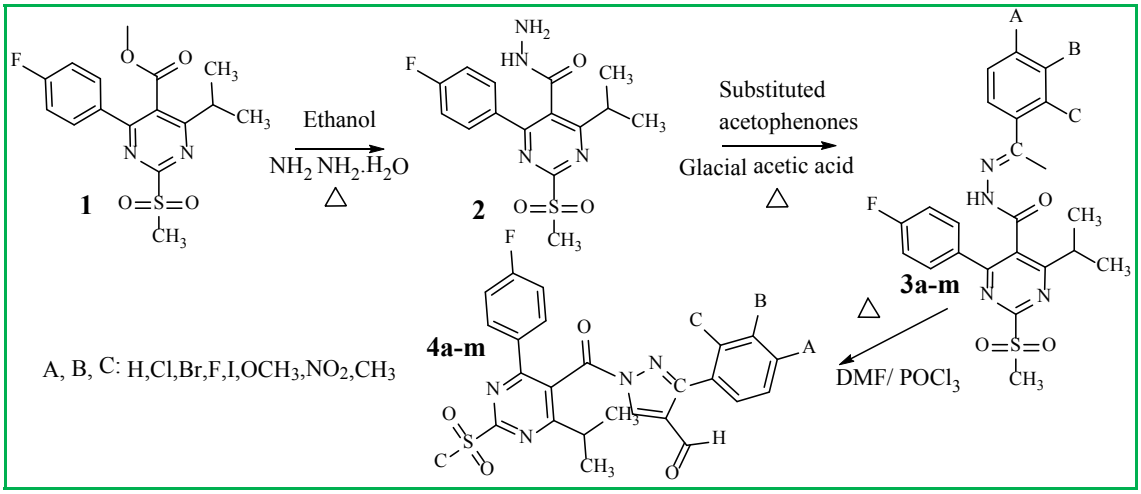


**Scheme 1.** General route for the synthesis of pyrazole carbaldehydes (4a-m).

**Table 1**
Functional unit details of reactant A, B, and C.

| S.NO | Reactant (Substituted acetophenone) | | | Product |
|---|---|---|---|---|
| | A | B | C | |
| 1 | Hydroxyl | H | H | **4a** |
| 2 | H | H | Fluoro | **4b** |
| 3 | Fluoro | H | H | **4c** |
| 4 | Bromo | H | H | **4d** |
| 5 | H | Bromo | H | **4e** |
| 6 | Methyl | H | H | **4f** |
| 7 | Chloro | H | H | **4g** |
| 8 | H | Chloro | H | **4h** |
| 9 | Hydrogen | H | H | **4i** |
| 10 | H | Methoxy | H | **4j** |
| 11 | H | H | Methoxy | **4k** |
| 12 | Nitro | H | H | **4l** |
| 13 | H | Nitro | H | **4m** |

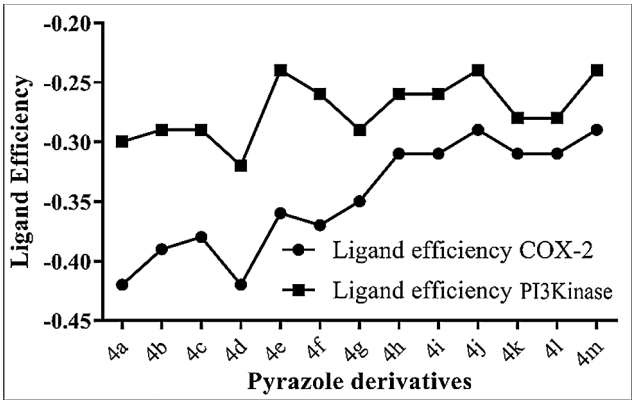


**Fig. 4.** Ligand efficiency comparison of pyrazoles **4a-m** against COX-2 and PI3Kinase.

treatment of **2** with substituted acetophenones in the presence of catalytic amount of glacial acetic acid. Further, Vilsmeier- Haack reaction of compounds **3a-m** at 70 °C for 8-10hrs yielded pyrazole carbaldehydes **4a-m** in 65–70%. All the compounds are crystalline solids having off-white to pale yellow in color. The compounds are stable in ordinary conditions and are insoluble in water and common organic solvents, but readily soluble in DMF and DMSO.

Table 1 displays the functional unit substituents details at A, B, and C positions of acetophenone. The novel pyrazoles **4a-m** obtained were well characterized through all major analytical techniques such as $^{1}$H NMR, $^{13}$C NMR, FTIR, LC-MS, and HRMS. For the biological assays, pyrazole compounds **4a-m** were taken in equal quantities and diluted in an equal volume of DMSO. The concentrations were in $10^{-1}$–$10^{-8}$ (μg/mL).

**Table 2**
Molecular mechanistic values of pyrazoles (**4a-m**) obtained from molecular docking studies.

| Entity | Binding Energy (BE) | | | | Inhibitory constant (*ki*) nM | | Ranking | | Final Ranking* |
|---|---|---|---|---|---|---|---|---|---|
| | COX-2 | 1CHW | 4a-m Sum | Average | COX-2 | 1CHW | COX-2 | 1CHW | |
| 4a | −11.43 | −9.48 | −20.91 | −10.45 | 3.55 | 54.27 | 3 | 4 | 4 |
| 4b | −10.84 | −8.15 | −18.99 | −9.49 | 11.34 | 64.17 | 7 | 8 | 9 |
| 4c | −10.78 | −7.89 | −18.67 | −9.33 | 12.54 | 89.78 | 8 | 12 | 10 |
| 4d | −11.88 | −10.15 | −22.03 | −11.01 | 3.24 | 18.49 | 2 | 3 | 2 |
| 4e | −10.64 | −8.64 | −19.28 | −9.64 | 15.91 | 86.47 | 9 | 6 | 6 |
| 4f | −11.92 | −10.95 | −22.87 | −11.43 | 3.02 | 9.88 | 1 | 1 | 1 |
| 4 g | −10.85 | −8.34 | −19.19 | −9.59 | 11.15 | 79.37 | 5 | 7 | 8 |
| 4 h | −10.48 | −7.91 | −18.39 | −9.19 | 20.09 | 91.48 | 10 | 12 | 11 |
| 4i | −10.85 | −8.17 | −19.02 | −9.51 | 11.07 | 96.43 | 5 | 9 | 7 |
| 4j | −9.63 | −6.84 | −16.47 | −8.23 | 30.08 | 112.48 | 12 | 13 | 13 |
| 4k | −10.79 | −9.14 | −19.93 | −9.96 | 12.4 | 64.25 | 6 | 5 | 5 |
| 4l | −10.99 | −10.22 | −21.21 | −10.60 | 9.8 | 18.65 | 4 | 2 | 3 |
| 4m | −10.17 | −8.07 | −18.24 | −9.12 | 24.85 | 68.34 | 11 | 10 | 12 |
| (BE) Sum | −141.2 | −113.9 | *Based on the sum and average values of binding energy (kcal/mol) | | | | | | |
| Average | −10.87 | −8.77 | | | | | | | |

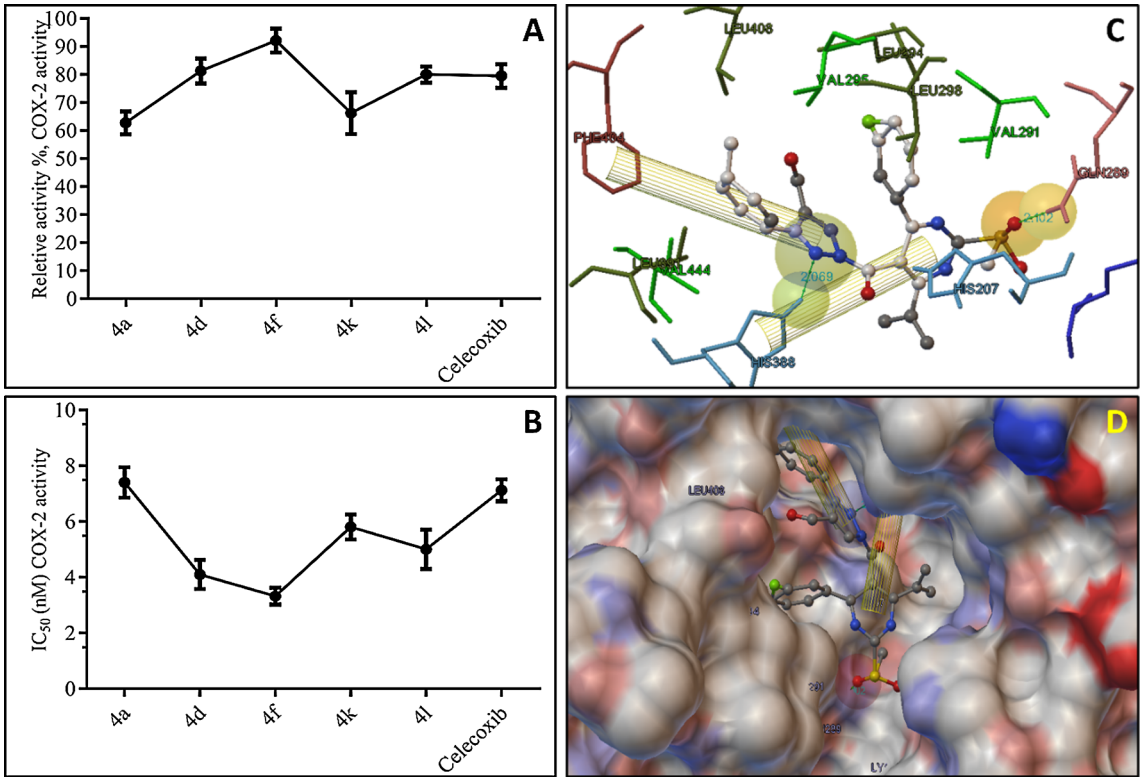


**Fig. 5.** The molecular resemblance of *in silico* and *in vitro* COX-2 inhibition studies of pyrazole compounds **4a**, **4d**, **4f**, **4k,** and **4l**. Note: All the experimental result values are obtained from four repeated assays (n = 4); **4A**. COX-2 relative % inhibition activity results; **4B**. Obtained $IC_{50}$ values of pyrazoles in COX-2 inhibition studies; **4C**. Molecular interaction of compound 4f to COX-2 (PDB ID: 1CX2) and **4D**. 4f into the binding pocket of COX-2 (PDB ID: 1CX2).

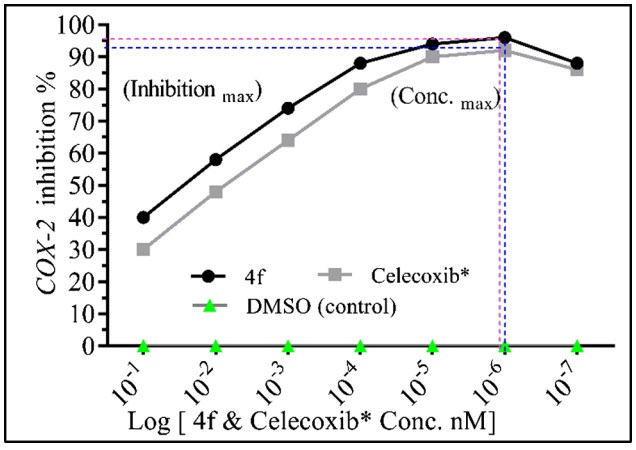


**Fig. 6.** Dose-response curve of pyrazole compound **4f** in the COX-2 inhibition *in vitro* studies.

### 3.2. Preliminary bioactivity screening results

Rather than blind bioactivity evaluations, a predicted and most probable bioactivity was focused. Online prediction tools such as Molinspiration (www.molinspiration.com/cgi-bin/properties) and PASSonline (www.pharmaexpert.ru/passonline/) were used for this preliminary bioactivity screening. Both tools are suggesting maximum and minimum possible activity scores. The most positive value was taken to determine the bioactivity through *in vitro* and *in silico* evaluations. The final structures of the pyrazole compounds **4a-m** were used to obtain their corresponding SMILE format using ChemDraw 15.0 version.

Fig. 3 illustrates the Molinspiration bioactivity score. Pyrazole derivatives showed Kinase inhibition (green line) and enzyme inhibition (black line) as the most potent activities possessed by them. PASSonline predictions suggested inflammation treatment and anticancer treatment potentials of pyrazole compounds. Combining these two results, and after recognizing COX-2 and PI3Kinase enzyme's involvement in both inflammation and cancer respectively, the present study was designed and executed to evaluate anti-inflammatory and anticancer studies through COX-2 and PI3Kinase inhibition potential evaluations.

### 3.3. Results of molecular docking studies

To go with economical, best compounds were screened based on the molecular mechanistic values obtained by individual pyrazoles **4a-m** from molecular docking studies to execute *in vitro* assays. The mode of Ligand-Receptor interactions was also assessed by docking studies. The major molecular mechanistic values such as least binding energy (kcal/mol), ligand efficiency and the inhibitory constant (*ki*) were taken into the account to rank the pyrazoles (**4a-m**) accordingly. Table 2 displaying the molecular mechanistic results of **4a-m** obtained from molecular docking studies. Based on the lowest binding energy values obtained by **4a-m**, they have been ranked in order to screen them for biological activities. Vertical and horizontal summing up and average calculations were made. From the individual ranking and overall ranking, pyrazole derivatives **4f**, **4d**, **4l**, **4a**, and **4k** were secured overall top 1 to 5 respectively and the same were dominated for COX-2 inhibition activities over PI3Kinase inhibition.

The binding energy summation and average assessments also ensured the same. From the sum value of −141.25 kcal/mol least binding energy against COX-2 inhibition and the anti-inflammatory activity potential of the present study pyrazoles **4a-m** was recognized (it was −113.95 kcal/mol against PI3Kinase). However, based on the best or top lowest binding energy values obtained for PI3Kinase was taken into account to screen the pyrazoles **4f**, **4d**, and **4l** to testify their PI3Kinase inhibition and anti-breast cancer effects.

**Table 3**
Druggability analysis of pyrazole compounds **4a-m.**

| Name | DCoef | MlogP | S + logP | S + logD | Ro5 | Ro5_Code | MWt | M_NO | T_PSA | HBDH |
|---|---|---|---|---|---|---|---|---|---|---|
| **4a** | 0.576 | 1.335 | 2.616 | 2.611 | 1 | Mw | 508.53 | 9 | 132.11 | 1 |
| **4b** | 0.579 | 2.175 | 3.237 | 3.237 | 1 | Mw | 510.52 | 8 | 111.88 | 0 |
| **4c** | 0.579 | 2.175 | 3.211 | 3.211 | 1 | Mw | 510.52 | 8 | 111.88 | 0 |
| **4d** | 0.564 | 2.377 | 3.23 | 3.23 | 1 | Mw | 571.43 | 8 | 111.88 | 0 |
| **4e** | 0.564 | 2.377 | 3.319 | 3.319 | 1 | Mw | 571.43 | 8 | 111.88 | 0 |
| **4f** | 0.567 | 2.276 | 3.421 | 3.421 | 1 | Mw | 506.55 | 8 | 111.88 | 0 |
| **4g** | 0.569 | 2.276 | 3.323 | 3.323 | 1 | Mw | 526.97 | 8 | 111.88 | 0 |
| **4h** | 0.569 | 2.276 | 3.304 | 3.304 | 1 | Mw | 526.97 | 8 | 111.88 | 0 |
| **4i** | 0.581 | 2.074 | 3.045 | 3.045 | 0 | < None > | 492.53 | 8 | 111.88 | 0 |
| **4j** | 0.562 | 1.537 | 3.092 | 3.092 | 1 | Mw | 522.55 | 9 | 121.11 | 0 |
| **4k** | 0.562 | 1.537 | 3.138 | 3.138 | 1 | Mw | 522.55 | 9 | 121.11 | 0 |
| **4l** | 0.567 | 1.978 | 3.028 | 3.028 | 2 | Mw; NO | 537.52 | 11 | 157.7 | 0 |
| **4m** | 0.567 | 1.978 | 2.792 | 2.792 | 2 | Mw; NO | 537.52 | 11 | 157.7 | 0 |

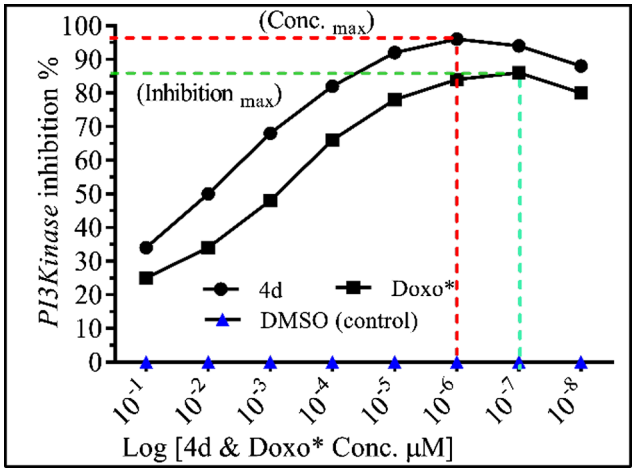


**Fig. 7.** Dose-response curve of compound 4f in the PI3Kinase inhibition assessment.

The other dimension that was taken to consider the drug efficacy of pyrazoles **4a-m** was ligand efficiency that was calculated by the binding energy per atom of a drug candidate/ligand to its corresponding receptor (most often an enzyme) [41]. Ligand efficiency usually considered as one of the key measurement in drug discovery and development researches. Because ligand efficiency measurement efficiently contributing in the small molecule drug efficacy validations through narrowing a lead compound's drug inevitability with optimal combinations of pharmacological and physicochemical properties [41]. Fig. 4 illustrates the obtained ligand efficiency and clearly indicates the selectivity of bioactivity potentials of **4a-m** against COX-2 inhibition (−0.30 to −0.42) than PI3Kinase inhibition (−0.22 to −0.33).

### 3.4. Enzyme inhibition study results – COX-2 inhibition studies

The COX-2 inhibition was measured by calculating the oxidation level of TMPD with and without the presence of COX-2 in the reaction mixture. To optimize the $C_{max}$, $T_{max}$, and $V_{max}$ the compounds experimented at various concentrations at different time intervals. According to Fig. 4, among the pyrazole compounds **4a**, **4d**, **4f**, **4k** and **4l**, compound **4f** was found to have dominated activity potentials (about 92% relative activity and lowest $IC_{50}$ 3.5 nM) (Fig. 5A and B).

At the same time, all the compounds were showed almost equal or higher activity when compared to the standard, Celecoxib. In fact, a concentration-dependent activity was recognized from the individual compound activity optimization assessments (Fig. 6 displays the dose-responsive curve of most effective pyrazole compound **4f**). To ensure this inhibition activity or to understand the mechanistic interaction mode of compound 4f and COX-2, we just extracted the molecular docking interaction image (Fig. 4C and D). As anticipated, there were two hydrogen bonds were formed between the key amino acid residues His388 and Gln289 which actively available in the corresponding catalytic site of COX-2. In addition, there were two π-π interactions (non-covalent type) also ensured the firm interaction to have expected drug efficacy or inhibitory potentials. Table 3 illustrates the druggability values of compounds **4a-m**.

### 3.5. Results of PI3 Kinase inhibition activity assay

Within PI3K/AKT/mTOR pathway there are numerous constituents, inhibition of which may result in cancer destruction [48]. In this study, as the bioactivity suggested and the same was confirmed through molecular docking studies, compounds **4a**, **4d**, **4f,** and **4l** were evaluated for their PI3Kinase inhibitory potentials. This evaluation was also considered to screen the best compounding **4a**, **4d**, **4f,** and **4l** to experimentally assess the anti-breast cancer potential as well as cytotoxicity effect as a representative compound among **4a-m**. The activity of PI3Kinase inhibition was dose-dependent (Fig. 7).

The determination of $V_{max}$, $T_{max,}$ and $C_{max}$ necessary for the maximum drug efficacy of compounds **4a**, **4d**, **4f,** and **4l**. Fig. 8, illustrates the resemblance of the molecular interaction of pyrazoles (**4a-m**) to PI3kinase. In the assay, compound **4f** showed a dominant activity with a great margin while comparing the standard doxorubicin. With highest relative percentage activity, compounds **4d** and **4l** got their attraction to evaluate their cytotoxicity potentials.

### 3.6. Cytotoxicity effects of representative compound 4d

The cytotoxicity or the anticipated anti-breast cancer effect of most potent PI3Kinase inhibitor 4d was assessed through the relative percentage activity and $IC_{50}$ value (n = 4). Doxorubicin was served as the standard drug. The relative percentage of 4d (91.5 ± 1.28) was higher than doxorubicin (86.2 ± 1.54) and the $IC_{50}$ was 0.25 ± 0.012 µM and 0.95 ± 0.025. Fig. 9 indicates the hourly changes measured for 4d after treating it to MCF-7 (breast cancer epithelial) and MCF-10 (normal breast epithelial) cell lines up to 4 h observations.

### 3.7. Drug efficacy of 4a-m through ADMET predictions

To assess the drug efficacy of the present study pyrazoles **4a-m**, we predicted the ADMET potentials using MedChem Designer (https://www.simulations-plus.com/software/medchem-designer/). Except for the molecular weight, remaining all categories was adopted to the Lipinski's 5 rule [49]. The solubility and the lipophilicity (LogP and LogD) of the pyrazoles **(4a-m)** were on the limit to adopt the rule.

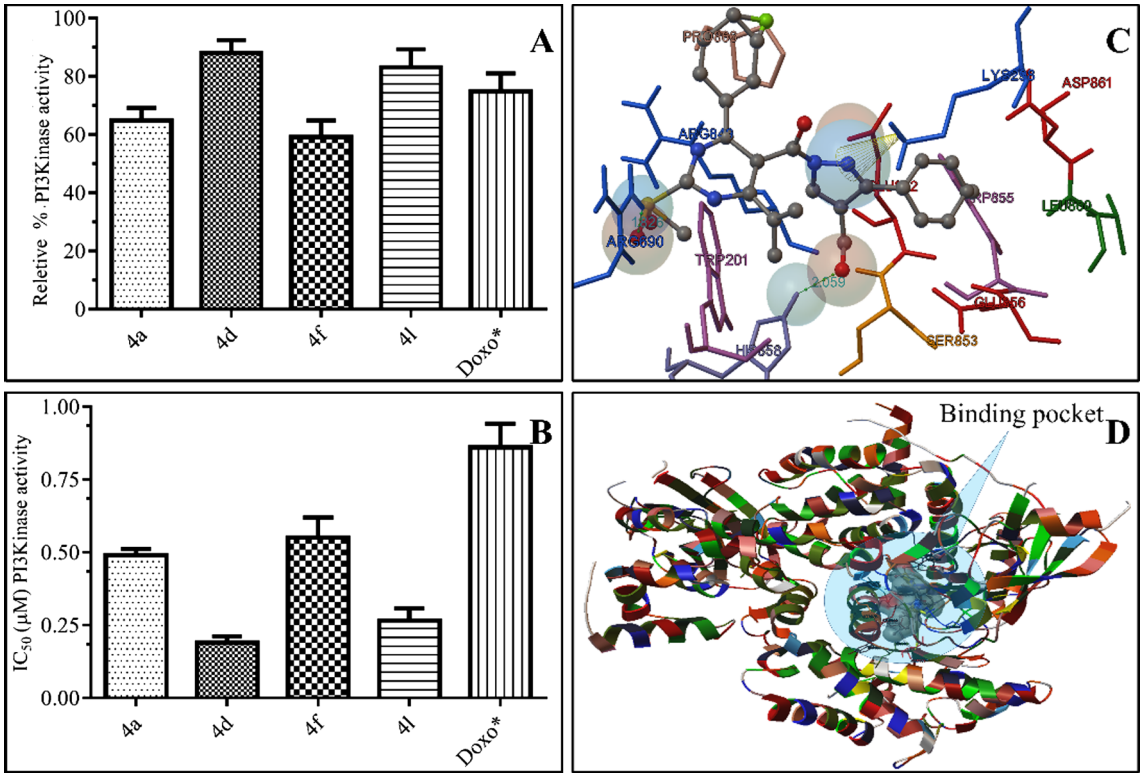


**Fig. 8.** The molecular resemblance of *in silico* and *in vitro* PI3Kinase inhibition studies of pyrazole compounds **4a**, **4d**, **4f**, and **4l**. Note: All the experimental result values are obtained from four repeated assays (n = 4); **6A**. COX-2 relative % inhibition activity results; **6B**. Obtained $IC_{50}$ values of pyrazoles in COX-2 inhibition studies; **6C**. Molecular interaction of compound **4d** to PI3Kinase (PDB ID: 1CHW) and **6D**. **4d** into the binding pocket of PI3Kinase (PDB ID: 1CHW).

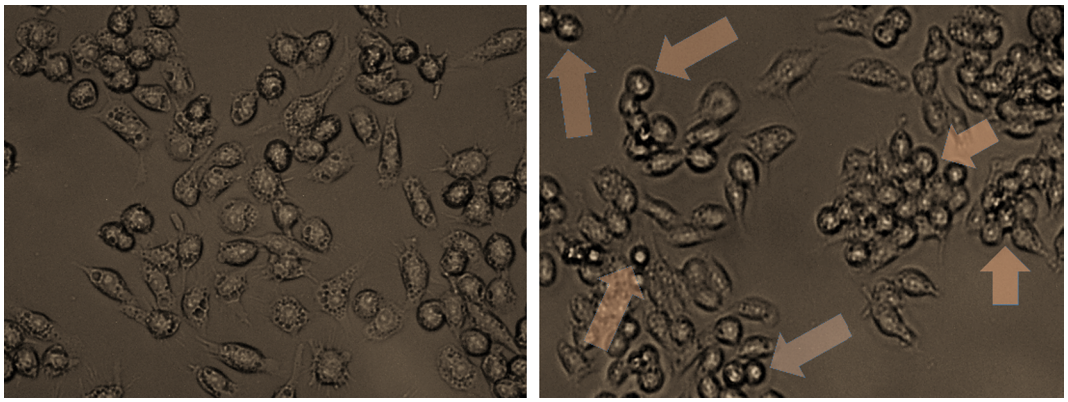

**Fig. 9.** Drug candidate treatment effects on normal epithelial cells (Left – MCF -0 cell lines) and breast cancer (Right – MCF-7 breast cancer epithelial).

DiffCoef– Differential co-efficient; S + logD − logD at user-specified pH (default 7.4); MlogP - Moriguchi estimation of logP; HBDH - Number of Hydrogen bond donor protons; M_NO - Total number of Nitrogen and Oxygen atoms; RuleOf5 (RO5) - Lipinski's Rule of Five: a score indicating the number of potential problems a structure might have with passive oral absorption; RuleOf5_Code - Lipinski's Rule of Five codes: LP = logP; Hb = number of Hydrogen bond donor protons; Mw = molecular weight; NO = number of Nitrogen- and Oxygen-based Hydrogen bond acceptors.

Table 3 illustrates the obtained ADMET values of **4a-m**. Most importantly, the obtained differential co-efficient values are highly suggesting the most possible druggability probabilities of almost all pyrazoles (**4a-m**). Even though almost all compounds are violating the Lipinski's 5 rule through the molecular weight, we could consider all these compounds as candidate drugs against the proposed activity here. Because a small molecule drug falls under the molecular weight of less than 900 Da [50].

## 4. Conclusion

In the present study, a wide range of substituted pyrazoles was synthesized and characterized through standard analytical techniques. The compound's exact bioactivity was predicted through various bioinformatics tools. The predicted COX-2 inhibition (anti-inflammatory effects) and PI3Kinase inhibition (anti-breast cancer effects) were determined through various *in vitro* assays for the top-ranked pyrazoles in the bioactivity prediction as well as in molecular docking studies. In the end, pyrazole moieties **4f** and **4d** were adjudged as the future anti-inflammatory and anti-breast cancer drugs.

## Acknowledgment

The authors are deeply acknowledging Research and Development Centre, Bharathiar University, Coimbatore - 641046, India.

## Appendix A. Supplementary material

Supplementary data to this article can be found online at https://doi.org/10.1016/j.bioorg.2019.02.003.

## References


[1] P.D. Leeson, B. Springthorpe, The influence of drug-like concepts on decision-making in medicinal chemistry, Nature Rev. Drug Discovery 6 (2007) 881–890.
[2] D.F. Veber, S.R. Johnson, H.Y. Cheng, B.R. Smith, K.W. Ward, K.D. Kopple, Molecular properties that influence the oral bioavailability of drug candidates, J. Med. Chem. 45 (2002) 2615–2623.
[3] M.R. Arkin, J.A. Wells, Small-molecule inhibitors of protein-protein interactions: progressing towards the dream, Nature Rev. Drug Discovery 3 (2004) 301–317.
[4] D.D. Nwibo, C.A. Levi, M.I. Nwibo, Small molecule drugs; down but not out: a future for medical research and therapeutics, IOSR J. Dental Medical Sci. (IOSR-JDMS) 14 (2015) 70–77.
[5] A. Tuha, A.A. Bekhit, Y. Seid, Screening of some pyrazole derivatives as a promising antileishmanial agent, Afr. J. Pharm. Pharmacol. 11 (2017) 32–37.
[6] M.J. Naim, O. Alam, F. Nawaz, M.J. Alam, P. Alam, Current status of pyrazole and its biological activities, J. Pharm. Bioallied Sci. 8 (2016) 2–17, https://doi.org/10.4103/0975-7406.171694.
[7] A. Ansari, A. Ali, M. Asif, Shamsuzzaman, Review: biologically active pyrazole derivatives, New J. Chem. 41 (2017) 16–41.
[8] R.S. Kumar, I.A. Arif, A. Ahamed, A. Idhayadhulla, Anti-inflammatory and antimicrobial activities of novel pyrazole analogs, Saudi J. Biol. Sci. 23 (2016) 614–620.
[9] A.M. Mohamed, W.A. El-Sayed, M.A. Alsharari, H.R. Al-Qalawi, M.O. Germoush, Anticancer activities of some newly synthesized pyrazole and pyrimidine derivatives, Arch. Pharm. Res. 36 (2013) 1055–1065.
[10] H. Kumar, D. Saini, S. Jain, N. Jain, Pyrazole scaffold: a remarkable tool in the development of anticancer agents, Eur. J. Med. Chem. 70 (2013) 248–258.
[11] M.S. Christodoulou, S. Liekens, K.M. Kasiotis, S.A. Haroutounian, Novel pyrazole derivatives: synthesis and evaluation of the anti-angiogenic activity, Bioorg. Med. Chem. 18 (2010) 4338–4350.
[12] A.E. Rashad, M.I. Hegab, R.E. Abdel-Megeid, J.A. Micky, F.M. Abdel-Megeid, Synthesis and antiviral evaluation of some new pyrazole and fused pyrazolopyrimidine derivatives, Bioorg. Med. Chem. 16 (2008) 7102–7106.
[13] D. Dias, B.S. Pacheco, W. Cunico, L. Pizzuti, C.M. Pereira, Recent advances on the green synthesis and antioxidant activities of pyrazoles, Mini. Rev. Med. Chem. 14 (2015) 1078–1092.
[14] M.A. Bhat, A.F. Ahmed, Z.H. Wen, M.A. Al-Omar, H.A. Abdel-Aziz, Synthesis, anti-inflammatory and neuroprotective activity of pyrazole and pyrazolo[3,4-d]pyridazine bearing 3,4,5-trimethoxyphenyl, Med. Chem. Res. 26 (2017) 1557–1566.
[15] P.A. Datar, S.R. Jadhav, Design and synthesis of pyrazole-3-one derivatives as hypoglycaemic agents, Int. J. Med. Chem. 2015 (2015) 670181.
[16] S. Levent, B. Çalışkan, M. Çiftçi, Y. Özkan, I. Yenicesu, H. Ünver, E. Banoglu, Pyrazole derivatives as inhibitors of arachidonic acid-induced platelet aggregation, Eur. J. Med. Chem. 64 (2013) 42–53.
[17] S. Salzano, P. Checconi, E.M. Hanschmann, C.H. Lillig, L.D. Bowler, P. Chan, D. Vaudry, M. Mengozzi, L. Coppo, S. Sacre, K.R. Atkuri, B. Sahaf, L.A. Herzenberg, L.A. Herzenberg, L. Mullen, P. Ghezzi, Linkage of inflammation and oxidative stress via the release of glutathionylated peroxiredoxin-2, which acts as a danger signal, PNAS 111 (2014) 12157–12162.
[18] T. Hussain, B. Tan, Y. Yin, F. Blachier, M.C.B. Tossou, N. Rahu, Oxidative stress and inflammation: what polyphenols can do for us? Oxid. Med. Cell. Longevity 2016 (2016) 7432797, https://doi.org/10.1155/2016/7432797.
[19] A. Manikandan, S. Ravichandran, K.I. Sathiyanarayanan, A. Sivakumar, Efficacy and rationale of 2-(4-phenylquinolin-2-yl) phenols as COX-2 inhibitors; an approach to emergent the small molecules as the anti-inflammatory and analgesic therapeutics, Inflammopharmacology 25 (2017) 621–631.
[20] M.R. Kumar, A. Manikandan, V.V. Dhayabaran, Synthesis, characterization and molecular evaluation of substituted indoline based dihydroxy-thiocarbamides as selective COX-2 inhibitors, J. Heterocyclic Chem. 55 (2018) 1658–1668.
[21] E. Ricciotti, G.A. FitzGerald, Prostaglandins and inflammation, Arterioscler Thromb Vasc Biol. 31 (2011) 986–1000.
[22] P.L. McCormack, Celecoxib: a review of its use for symptomatic relief in the treatment of osteoarthritis, rheumatoid arthritis, and ankylosing spondylitis, Drugs 71 (2011) 2457–2489.
[23] K.S. Na, K.J. Lee, J.S. Lee, Y.S. Cho, H.Y. Jung, Efficacy of adjunctive celecoxib treatment for patients with the major depressive disorder: a meta-analysis, Prog. Neuro-Psychopharmacol. Biol. Psychiatry. 48 (2014) 79–85.
[24] P. Thangarasu, S. Thamarai Selvi, A. Manikandan, Unveiling novel 2-cyclopropyl-3-ethynyl-4-(4-fluorophenyl)quinolines as GPCR ligands via PI3-kinase/PAR-1 antagonism and platelet aggregation valuations; development of a new class of anticancer drugs with thrombolytic effects, Bioorg. Chem. 81 (2018) 468–480.
[25] A. Manikandan, A. Sivakumar, Molecular explorations of substituted 2-(4-phenyl quinoline-2-yl) phenols as phosphoinositide 3-kinase inhibitors and anticancer agents, Cancer Chemother. Pharmacol. 79 (2017) 389–397.
[26] A. Kadirappa, A. Manikandan, R.S. Mundre, A.A. Napoleon, Copper-catalyzed quinoline derivatives evaluated as a new class of anticancer agents: design, synthesis and molecular validations, J. Heterocyclic Chem. 55 (2018) 1669–1677.
[27] V.P. Muralidharan, M. Alagumuthu, S. Arumugam, S.K. Iyer, Molecular substantiation and drug efficacy of relatively high molecular weight S-BINOLs; appraised as breast cancer medication and PI3Kinase inhibitors, J. Heterocyclic Chem. 55 (2018) 1339–1345.
[28] M.R. Kumar, A. Manikandan, V.V. Dhayabaran, N-substituted hydroxynaphthalene imino-oxindole derivatives as a new class of pi3-kinase inhibitor and breast cancer drug: molecular validation and structure-activity relationship studies, Chem Biol Drug Des. 91 (2018) 277–284.
[29] P. Liu, H. Cheng, T.M. Roberts, J.J. Zhao, Targeting the phosphoinositide 3-kinase pathway in cancer, Nat Rev Drug Discov. 8 (2009) 627–644.
[30] E. Paplomata, R. O'Regan, The PI3K/AKT/mTOR pathway in breast cancer: targets, trials, and biomarkers, Ther Adv Med Oncol. 6 (2014) 154–166.
[31] J. Yu, Y. Zhang, J. McIlroy, T.R. Nikolic, G.A. Orr, I.M. Backer, Regulation of the p85/p110 phosphatidylinositol 3'-kinase: stabilization and inhibition of the p110alpha catalytic subunit by the p85 regulatory subunit, Mol Cell Biol. 18 (1998) 1379–1387.
[32] G. Multhoff, M. Molls, J. Radons, Chronic inflammation in cancer development, Front Immunol. 2 (98) (2012), https://doi.org/10.3389/fimmu.2011.00098 (2012).
[33] L.M. Coussens, Z. Werb, Inflammation and cancer, Nature 420 (2002) 860–867.
[34] D.G. DeNardo, L.M. Coussens, Inflammation and breast cancer. Balancing immune response: crosstalk between adaptive and innate immune cells during breast cancer progression, Breast Cancer Res. 9 (2007) 212.
[35] A. Manikandan, P.M. Vivek, M. Andrew, M.H. Ahmed, K.I. Sathiyanarayanan, A. Sivakumar, Computational approaches to develop isoquinoline based antibiotics through DNA gyrase inhibition mechanisms unveiled through antibacterial evaluation and molecular docking, Mol. Inf. (2018), https://doi.org/10.1002/minf.201800048.
[36] A. Manikandan, A. Sivakumar, Molecular docking, discovery, synthesis, and pharmacological properties of new 6-substituted-2-(3-phenoxyphenyl)-4-phenyl quinoline derivatives; an approach to developing potent DNA gyrase inhibitors/antibacterial agents, Bioorganic Med. Chem 25 (2017) 1448–1455.
[37] A. Manikandan, S. Ravichandran, K. Kumaravel, A. Sivakumar, R. Priya, Molecular docking and in vitro evaluations of *Hippocampus trimaculatus* (seahorse) extracts as anti-inflammatory compounds, Int. J. Bioinform. Res. Appl. 12 (2016) 355–371.
[38] A. Manikandan, K.I. Sathiyanarayanan, A. Sivakumar, Molecular docking, design, synthesis, in vitro antioxidant and anti-inflammatory evaluations of new isoquinoline derivatives, Int J Pharm Pharm Sci. 7 (2015) 200–208.
[39] A. Manikandan, P. Moharil, M. Sathiskumar, C. Muñoz-Garay, A. Sivakumar, Therapeutic investigations of novel Indoxyl-based indolines: a drug target validation and structure-activity relationship of angiotensin-converting enzyme inhibitors with cardiovascular regulation and thrombolytic potential, Eur. J. Med. Chem. 141 (2017) 417–426.
[40] I.D. Kuntz, K. Chen, K.A. Sharp, P.A. Kollman, The maximal affinity of ligands, Proc Natl Acad Sci U S A. 96 (1999) 9997–10002.
[41] C. Abadzapatero, J. Metz, Ligand efficiency indices as guideposts for drug discovery, Drug Discovery Today 10 (2005) 464–469.
[42] R.A. Copeland, J.M. Williams, J. Giannaras, S. Nurnberg, M. Covington, D. Pinto, S. Pick, J.M. Trzaskos, Mechanism of selective inhibition of the inducible isoform of prostaglandin G/H synthase, Proc Natl Acad Sci U S A. 91 (1994) 11202–11206.
[43] N. Petrovic, M. Murray, Using N, N, N', N'-tetramethyl-p-phenylenediamine (TMPD) to assay cyclooxygenase activity in vitro, Methods Mol Biol. 594 (2010) 129–140.
[44] W. Lemmo, Potential interactions of prescription and over-the-counter medications having antioxidant capabilities with radiation and chemotherapy, Int. J. Cancer 137 (2014) 2525–2533.
[45] M.R. Kumar, A. Manikandan, D.V. Violet, Synthesis, characterization and molecular evaluation of substituted indoline based dihydroxy-thiocarbamides as selective COX-2 inhibitors, J. Heterocyclic Chem. 55 (2018) 1658–1668, https://doi.org/10.1002/jhet.3201.
[46] C.A. Anosike, O. Obidoa, L.U. Ezeanyika, Membrane stabilization as a mechanism of the anti-inflammatory activity of methanol extract of garden egg (Solanum aethiopicum), Daru. 20 (2012) 76, https://doi.org/10.1186/2008-2231-20-76.
[47] K.K. Hirai, T.O. Ishiba, H.K. Koike, M.S Watanabe, Pyrimidine Derivatives. Patent Number: US RE37,314 E (Reissued U.S. Pat. No. 5,260,440, issued Nov. 8, 1993).
[48] J.E. Kurtz, I. Ray-Coquard, PI3 kinase inhibitors in the clinic: an update, Anticancer Res. 32 (2012) 2463–2470.
[49] C.A. Lipinski, F.F. Lombardo, B.W. Dominy, P.J. Feeney, Experimental and computational approaches to estimate solubility and permeability in drug discovery and development settings, Adv. Drug Deliv. Rev. 46 (2001) 3–26.
[50] M.J. Macielag, Chemical properties of antibacterials and their uniqueness, in: T.J. Dougherty, M.J. Pucci (Eds.), Antibiotic Discovery and Development, Springer, Boston, MA, 2012, pp. 801–802 ISBN 978-1-4614-1400-1.